



TECHNICAL ARTICLE

Fabrication, Tensile, and Hardness Properties of Novel Cast WC-Reinforced 304 Stainless Steel Composites

JUN DENG¹ and ZHAOYAO ZHOU^{1,2}

1.—Guangdong Key Laboratory for Processing and Forming of Advanced Metallic Materials, School of Mechanical and Automotive Engineering, South China University of Technology, Guangzhou 510640, China. 2.—e-mail: zhyzhou@scut.edu.cn

304 stainless steel powder, cast WC powder, and 304 close-grained stainless steel wire mesh were used as raw materials to prepare cast WC particle-reinforced 304 stainless steel composites. The composites were formed by rolling and sintering, and then re-rolling and re-sintering procedures were used to boost the performance of the composites. The effects of the mass fraction of cast WC in the powder, the sintering temperature, and the rolling deformation on the hardness, tensile properties, and fracture morphology of the composites were investigated. The results show that the hardness and yield strength of the composites positively correlated with all three process parameters, of which rolling reduction had the greatest influence. An increase in either temperature or cast WC content led to an undesirable clustering of cast WC particles, which led to brittle fracture locally in the material and reduced the tensile strength and plasticity of the composites. Moreover, the increase in rolling deformation helped to improve the strength and plasticity of the composites. For tensile properties, the optimum content of cast WC in the blended powder was 10 wt.%, the perfect sintering temperature was 1200°C, and the best rolling reduction was 35% in the range of parameters studied in this work.

INTRODUCTION

Compared with single metals, metal matrix composites combine the properties of matrix materials and reinforcements, possess high strength, high modulus, low density, and high wear resistance, and are widely used.^{1–6} As steel is one of the most widely used metals in various countries and fields around the world, the development of composite materials using it as a matrix has been given great importance.^{7,8} In recent decades, many scholars have conducted research in the field of particle-reinforced steel matrix composites. For example, Kang et al.⁹ prepared WC/18Ni-300 composites by selective laser melting. Jamaati et al.^{10,11} prepared steel matrix composites by a cumulative rolling process and investigated their mechanical properties and fracture behavior. Jain et al.¹² prepared steel matrix

composites by powder metallurgy and observed that the addition of YGA increased the density and hardness of the composites. Abenojar et al.¹³ prepared 27 groups of particle-reinforced 316L stainless steel composites using conventional powder metallurgical methods and investigated the effects of the sintering atmosphere and type of reinforcing particles on the hardness, density, tensile strength, and other properties of the composites. Guan et al.^{14,15} prepared PCS-316 composites using a semi-powder metallurgical method and investigated in detail the effect of PCS content on the mechanical properties. Lin¹⁶ prepared WC-304 stainless steel composites with different WC contents by direct laser alloying and investigated the effect of process conditions on the hardness and toughness of the composites.

Reinforcement particles are incorporated into the matrix material to produce particle-reinforced steel matrix composites by powder metallurgy,^{12–15} laser sintering,^{9,16} in-situ generation,^{17–19} and extrusion casting.^{20,21} The extrusion casting method is

(Received August 17, 2022; accepted December 16, 2022; published online January 23, 2023)

generally suitable for reinforcing particles with a density similar to that of the base material, while the laser sintering method is more demanding for the equipment and not conducive to mass production. Powder metallurgy is a simple process and often results in a composite material with a uniform distribution of reinforcement particles, so it is widely used;²² powder rolling is a method of powder forming suitable for large sizes and mass-production.

In contrast, there is relatively little published on the preparation of stainless steel matrix composites by powder rolling, or their mechanical properties. Therefore, a new way to prepare 304 stainless steel-based composites is proposed in this study: the composites are obtained by roll forming and vacuum sintering using reinforcement powder, 304 powder, and 304 steel wire mesh as raw materials, followed by re-rolling and re-sintering to improve the mechanical properties of the composites. Popular reinforcement particles for steel matrix composites include WC, TiC, Al_2O_3 , SiC, Si_3N_4 , and PCS,^{23,24} among which WC has better wettability with stainless steel,¹⁶ which is why WC was used as a reinforcement particle in this study. In addition, after preparing the composites, the effect of the process parameters during preparation on the hardness, tensile properties, and fracture mode of the composites was investigated in this paper.

MATERIALS AND METHODS

In this work, 400-mesh dense-grained 304 stainless steel wire mesh and 200-mesh 304 stainless steel powder were used as the base materials, and 200-mesh cast tungsten carbide powder was used for the reinforcing particles. Figure 1 shows the microscopic morphologies of the raw materials.

304 stainless steel powder with an average particle size of $75\ \mu m$ and cast tungsten carbide powder with an average particle size of approximately $75\ \mu m$ were mechanically mixed to produce six different WC-304 blends, where the mass fractions of the cast tungsten carbide particles were 0%, 5%, 10%, 15%, 20%, and 25%. Then, the mixed powder was spread on the stainless steel wire mesh and

passed through a two-roller cold rolling mill with a zero roller gap (powder spread thickness of 0.8 mm, roller diameter of 350 mm, and rolling force of 240 tons) under friction to obtain a thin cast WC-304 composite strip. Then, the cast WC-304 composite strip was folded 6 times and placed in a vacuum sintering furnace for vacuum sintering (WHS-20 vacuum sintering furnace); the cast WC-304 composite plate was then obtained. Next, to improve the mechanical properties of the composite plate, the cast WC-304 composite plate obtained after sintering was rolled to a certain thickness and subsequently placed in a vacuum sintering furnace for secondary sintering, with the same sintering process as the first to obtain the final cast WC-304 composite. The preparation process route is shown in Fig. 2, 3a shows the sintering temperature profile used for the vacuum sintering session. Twelve sets of samples were prepared using the preparation method shown in Fig. 2, and the process parameters for each set of examples are described in Table I.

All the samples were subjected to microhardness measurements, quasi-static uniaxial tensile tests, analysis of the physical phases and material surface, and analysis of the tensile fracture morphologies. The diffraction patterns of the samples were measured using an x-ray diffractometer (PANalytical polycrystalline x-ray diffractometer) to determine the phase composition of the sample (Cu target, $5\text{--}90^\circ$, $0.033^\circ/10\ s$). An environmental scanning electron microscope was used to view the surface micromorphology and tensile fractures of the pieces (FEI, Quanta 200, The Netherlands). A tensile test on cast WC-304 composite material was carried out at room temperature using a universal testing machine (Sanshi, Shenzhen) with a tensile specimen gauge of 15 mm and a strain rate setting of 0.5 mm/min. Five tensile specimens were used for each process parameter, and a total of 60 tensile specimens were used for tensile testing. The microhardness of the samples was tested using a digital micro Vickers hardness tester with a loading force of 300 g and a holding time of 15 s.

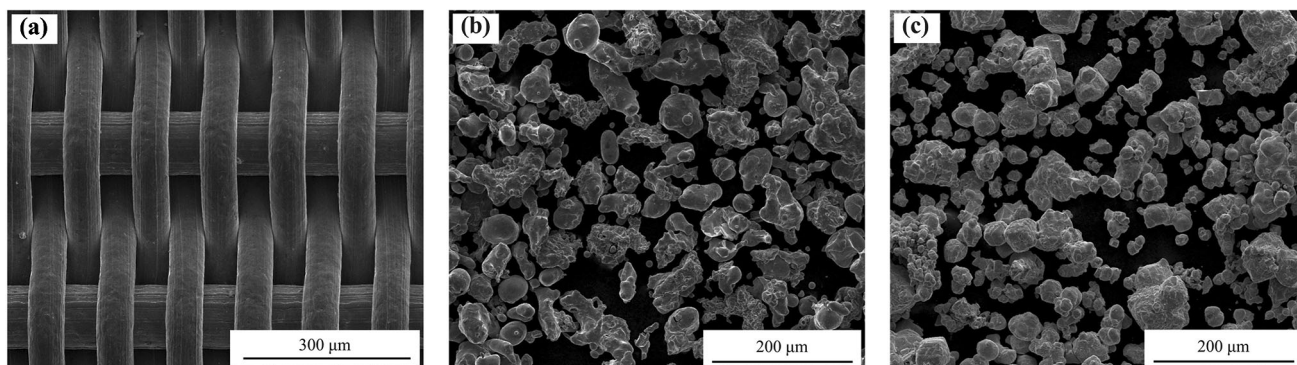


Fig. 1. Raw material morphology: (a) 304 wire mesh; (b) 304 powder; (c) cast WC powder.

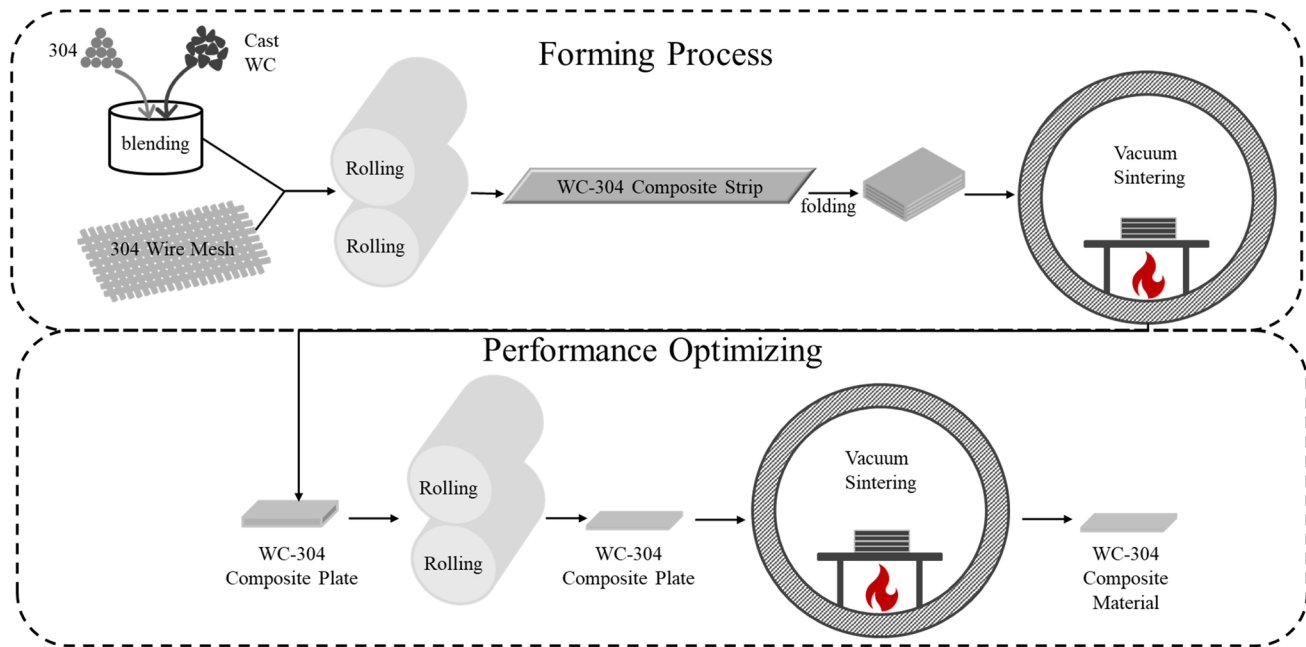


Fig. 2. Preparation process of cast WC-304 composites.

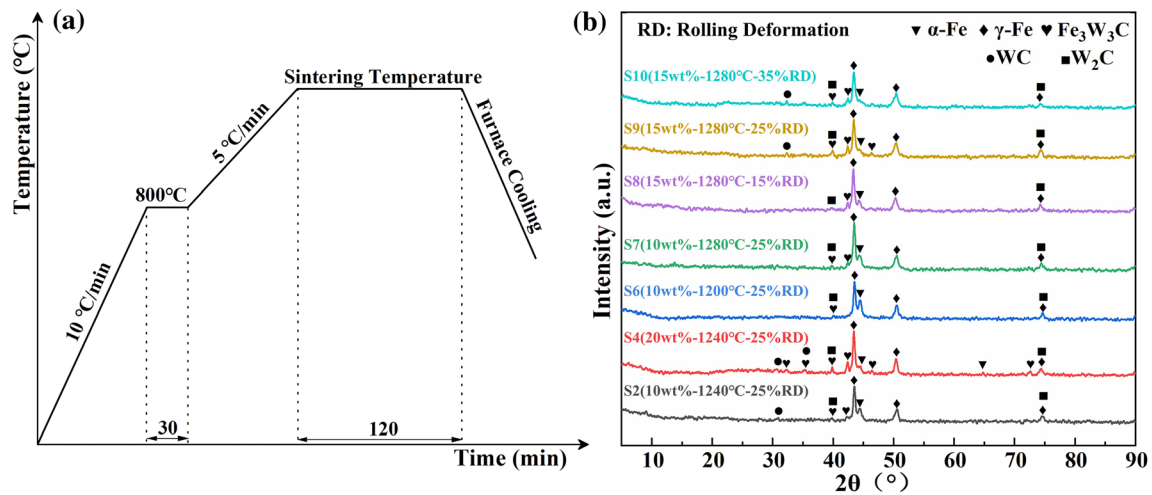


Fig. 3. (a) Sintering temperature curve and (b) XRD profiles of the seven specimens.

Table I. Fabrication parameters of eleven samples

Sample	Cast WC mass fraction (%)	Sintering temperature (°C)	Rolling deformation (%)
S0	0	1240	25
S1	5	1240	25
S2	10	1240	25
S3	15	1240	25
S4	20	1240	25
S5	25	1240	25
S6	10	1200	25
S7	10	1280	25
S8	15	1280	15
S9	15	1280	25
S10	15	1280	35
S11	10	1200	35

RESULTS AND DISCUSSION

Physical Phase Analysis

To determine the phase composition of the composites and investigate the effect of process parameters on the phases of the composites, XRD analysis was performed on S2, S4, S6, S7, S8, S9, and S10, and the x-ray diffraction patterns of the samples are shown in Fig. 3b. The greater the content of reinforcement particles in the sample, the greater the number of diffraction peaks. The composites consisted mainly of γ -Fe in a face-centered cubic lattice and α -Fe in a body-centered cubic lattice; this was because the raw material 304 stainless steel was austenitic stainless steel with a face-centered cubic structure, and the austenite was partially transformed into martensite with a body-centered cubic system after several cold rolling processes,²⁵ which was then reconverted to austenite during the subsequent high-temperature sintering and reheating process. When the holding time was over, the austenite transformed back to ferrite during cooling, resulting in the presence of both α - and γ -iron in the final composite.²⁶ When the mass fraction of cast WC in the powder reached 20% (S4), diffraction peaks representing $\text{Fe}_3\text{W}_3\text{C}$ could be observed as a result of the interdiffusion between W and C elements in the reinforced particles and Fe element in the stainless steel. In addition, the diffraction peaks represented by WC and W_2C can be seen in the diffractogram of sample 4. In samples with lower cast WC content than S4, the diffraction peaks corresponding to some phases were difficult to observe because the content of cast WC was lower than the limited resolution of the XRD equipment used. However, this does not mean that these phases were not present. In addition, the formation of the hard phase $\text{Fe}_3\text{W}_3\text{C}$ was beneficial to the microhardness and wear resistance of the composites.^{16,27,28}

Microstructure

Figure 4 shows the surface micromorphology of 304 stainless steel material and composites with different particle contents, while Fig. 4a shows the surface of 304 stainless steel. The composite surfaces with different cast WC contents in the blended powders are shown in Fig. 4b–f (S1–S5). When the mass fraction of reinforcing particles in the powder reached 10%, the reinforcing particles in the material started to appear in clusters. This became more pronounced as the concentration of reinforcing particles increased.

Figure 4g–i show the surface morphologies of the composites with process parameters of 10 wt.% cast WC, 25% rolling reduction and sintering temperatures of 1200 °C, 1240 °C, and 1280 °C (S6, S2, and S7), respectively. Although the three samples differed only in the sintering temperature, their surfaces differed considerably. As the sintering

temperature increased, the reinforcement particles on the surface became fewer and more unevenly distributed. The reason for this undesirable phenomenon is the aggregation of the reinforcement particles. It can be seen that the higher the sintering temperature, the more pronounced the accumulation of the reinforcement particles, making the number of reinforcement particles intuitively smaller and the particle size larger.

Figure 4j–l show the microscopic morphologies of the composites with different rolling reductions (S8–S10). As the figure shows, the increase in the rolling reduction was favorable to the dispersion of the reinforcing particles; the more extensive the rolling reduction was, the less aggregation of the reinforcement particles, making them dispersed in the matrix more uniformly and closer to their original size.

Tensile Properties of the Composites

Influence of Reinforcement Particle Content on the Tensile Properties

The cast WC content affects the tensile properties of the composites, including tensile strength, yield strength, and elongation. Figure 5 shows the tensile properties for materials corresponding to different ranges of cast WC (S0–S5). First, the stretching curve of the composite followed a generally consistent trend, with the entire stretching process divided into roughly three stages. The first stage was the elastic stage, where the stress–strain of the material satisfies Hooke's law and was represented as a straight line in the tensile curve and where the process occurred for a short period. It can then be seen that the material did not exhibit a significant yielding stage and went directly from the elastic stage to the plastic deformation stage. This phenomenon is consistent with the tensile behavior of powder mesh materials.²⁹ During the plastic deformation stage, the strength of the material increased considerably due to the work-hardening phenomenon that occurred at the same time as the deformation. The third stage was the fracture stage, which was reflected in the tensile curve as a significant reduction in stress in a short time, but this does not mean that the fracture of the composite was instantaneous. The composite material prepared by the above process had a certain number of pores, which led to stress concentration. In the plastic deformation stage, these pores began to expand into cracks, with a gradual increase in the deformation crack range or even with the appearance of crack interconnections. When damage accumulated to a certain extent, the material was wholly torn off under high tensile forces.²⁹

To more visually assess the effect of the reinforcement particle content on the tensile properties of the composites, the tensile strength, yield strength, and elongation of the composites with a range of reinforcement contents are shown in the

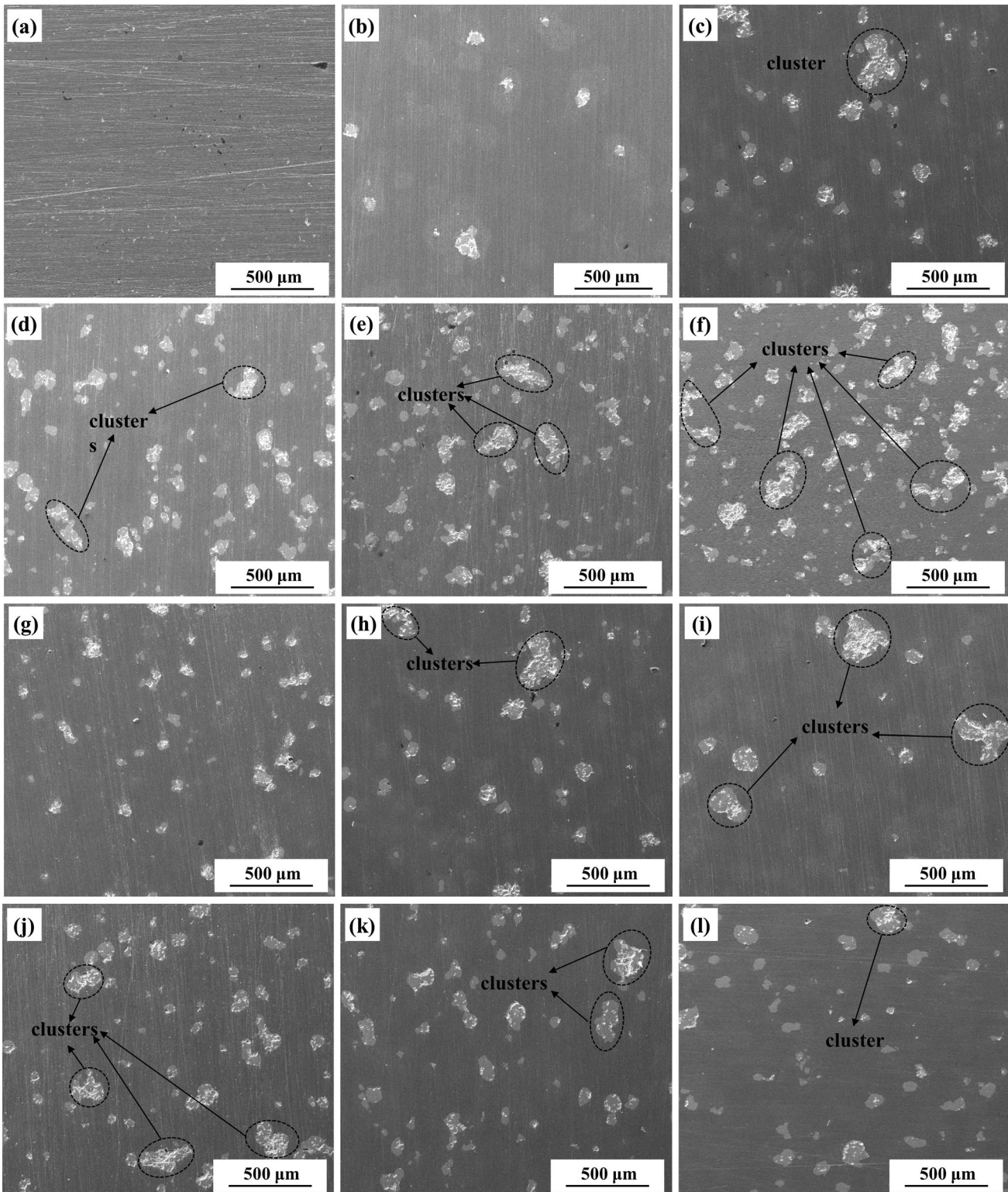


Fig. 4. Surface profile of the composites with different process parameters: (a)–(f) 0–25 wt.% cast WC, (g)–(i) 1200–1280 °C, and (j)–(l) 15–35% rolling reduction.

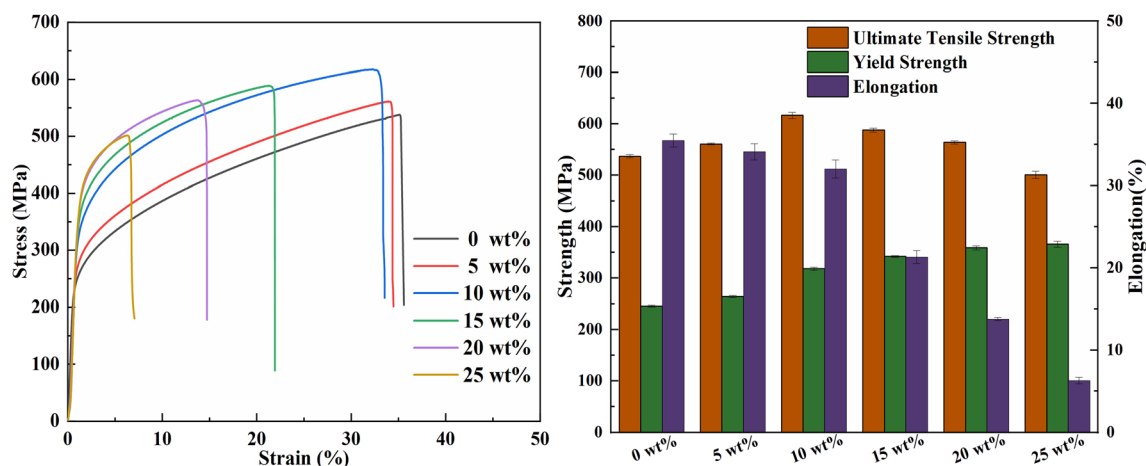


Fig. 5. Effect of the mass fractions of cast WC on tensile properties.

form of histograms in Fig. 5. As is evident, the yield strength of the composite continued to increase with increasing cast WC content, while the plasticity was reduced. Compared with S0 (0 wt.% cast WC), S5 (25 wt.% cast WC) displayed a 48.8% improvement in yield strength (246 MPa versus 366 MPa, respectively) and 82.3% reduction in plasticity (36% versus 6.3%). When the cast WC content increased from 0 wt.% to 10 wt.%, the tensile strength first increased from 537 MPa to 617 MPa; then, when the cast WC content gradually increased to 25%, the tensile strength gradually decreased to 501 MPa, showing a trend of rising first and then falling. The increase in tensile and yield strengths was because the reinforcement particles tended to be stiffer than the matrix, and the applied load was transferred from the matrix to the reinforcement, causing the reinforcement particles to withstand more stress. However, a reinforcement concentration that is too high causes a more pronounced cluster of reinforcement particles within the material, which in turn hurts the material's tensile strength.^{30–32} On the other hand, the reduction in elongation was due to the earlier onset of pore nucleation as the amount of reinforcement particles increased, further leading to an earlier material fracture time.³⁰ Overall, the best tensile properties of the composites were obtained when the mass fraction of cast WC in the powder was 10%.

Influence of Sintering Temperature on the Tensile Properties

To investigate the effect of sintering temperature on the tensile properties, tensile tests were carried out on composites with sintering temperatures of 1200 °C, 1240 °C, and 1280 °C (S6, S2, and S7), respectively. The engineering stress–strain curves and the effects of sintering temperature on the tensile strength, yield strength, and elongation of the composites are shown in Fig. 6. The yield strength of the material varied very little,

indicating that it was less affected by the sintering temperature; however, the tensile strength and elongation decreased as the sintering temperature increased. Specifically, when the firing temperature increased from 1200 °C to 1240 °C, the material's tensile strength decreased by 634–17 MPa, and the elongation fell from 41 to 32%. When the sintering temperature increased from 1240 °C to 1280 °C, the tensile strength had an 11.7% reduction (from 617 MPa to 545 MPa), and the elongation decreased from 32% to 16.5%. The tensile strength of the composite at 1200 °C was 16.3% higher than that of the material prepared at 1280 °C, and the elongation was 148.5% higher.

This seems to be contrary to the nature of conventional powder metallurgical materials. For general powder metallurgical materials, an increase in sintering temperature is conducive to better mechanical properties and plasticity of the material. A higher sintering temperature, on the one hand, can promote the growth of the sintering neck of the powder metallurgical material, thus achieving a better metallurgical bond. On the other hand, the increase in sintering temperature can promote the diffusion of atoms, which reduces the number of pores in the material, reduces the stress concentration phenomenon, and improves the material properties.^{33–35} However, for the present work, it can be seen from Fig. 4g–i that the sintering temperature had a dramatic effect on the distribution of reinforcement particles. As the sintering temperature increased, the aggregation of reinforcement particles in the composite became prominent, which had two significant consequences. First, the distribution of reinforcement particles was fairly uniform at the right temperature. Nevertheless, the presence of aggregation led to a concentration of reinforcement particles in one part of the area and a lack of reinforcement particles in another area, thus making the distribution of reinforcement particles in the material extremely non-uniform. The material in this state was more susceptible to damage than a

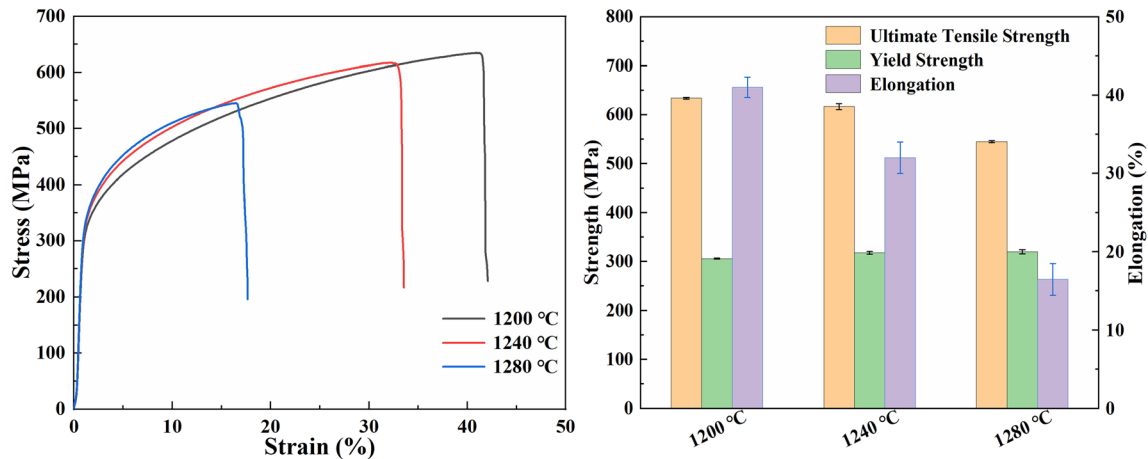


Fig. 6. Effect of sintering temperature on the tensile properties.

uniformly distributed particle-reinforced composite, which significantly reduced mechanical properties.³² Second, the gathering of reinforcement particles could be thought of as several small reinforcement particles coming together to form larger reinforcement particles, which was equivalent to using large reinforcement particles to prepare the composite, which also led to a reduction in the tensile strength of the material.³⁶ Therefore, for this study, the detrimental effects of particle clustering were much stronger than the advantages of increased sintering temperatures, leading to the results shown in Fig. 6. In summary, the difference in the particle distribution of the reinforcement brought by the difference in the sintering temperature had a tremendous effect on the tensile properties of the composite. It can be concluded that 1200 °C was the optimum temperature for preparing the composite.

Influence of Rolling Down on the Tensile Properties of the Composites

The tensile properties of the composites were investigated for three rolling reductions of 15%, 25%, and 35% (S8–S10). Figure 7 shows the engineering stress–strain curve and the effects of rolling deformation on the tensile properties of the composites.

It is clear that the effect of rolling reduction on the tensile properties was significant. The yield strength, tensile strength, and elongation at 35% thickness reduction were 387 MPa, 644 MPa, and 22.2%, respectively. These values increased by 19.8%, 31.7%, and 113.5%, respectively, compared with those of 15% thickness reduction, achieving a synergistic increase in the strength and toughness.

This phenomenon was not difficult to understand. First, the initial sintered cast WC-304 composite plate had many pores. In the process of stretching, these pores formed cracks due to stress concentration and eventually led to the fracture of the material, while a more significant amount of rolling down can reduce the pores in the material, greatly

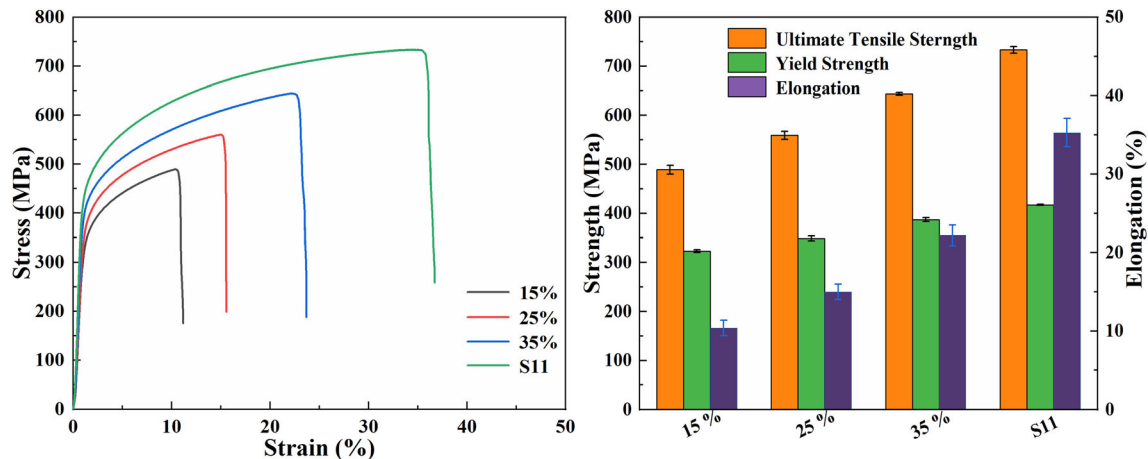


Fig. 7. Effect of rolling deformation on tensile properties.

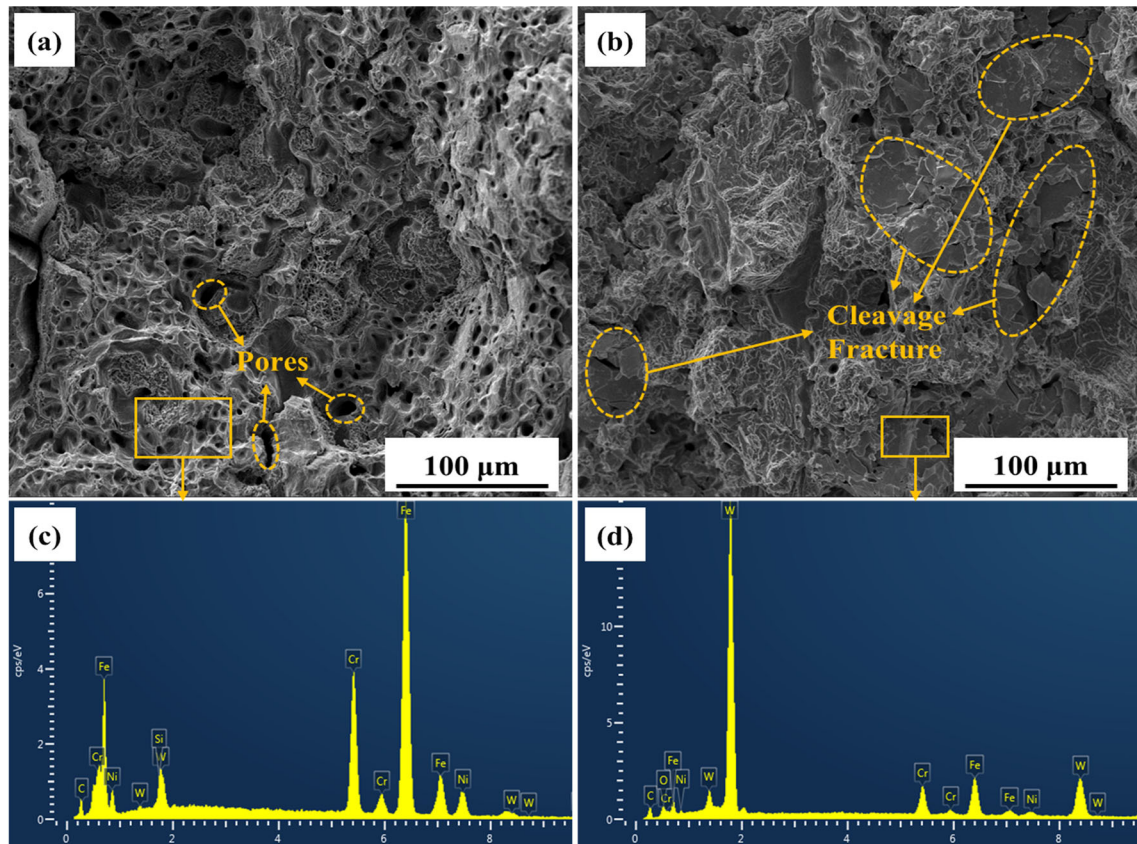


Fig. 8. Tensile fracture for different reinforcement concentrations: (a) 10 wt.%, (b) 25 wt.%, and (c, d), with EDS results for their respective yellow areas.

improving its strength. Second, cold rolling could play a role in refining the grain of stainless steel materials, thus improving the strength and hardness of the material,³⁷ although after secondary rolling the material can exhibit a reduction in plasticity due to work-hardening phenomena.³⁸ In this study, however, a sintering process was carried out after re-rolling, the same as the initial process. This process eliminated the work hardening caused by the previous cycle and resulted in a more compact material after re-rolling. The second sintering allowed the previous sinter necks to grow and form some new sinter necks. This process improved the plasticity and strength of the material so that after re-rolling and re-sintering, there was a synergistic increase in the strength and plasticity of the composite.

Combining the results of the effects of reinforcement concentration, sintering temperature, and rolling down on the tensile properties, it can be seen that for this study, the process parameters that resulted in the best tensile properties of the composites were 10 wt.% cast WC powder, 1200 °C sintering temperature, and 35% thickness reduction. The tensile properties of the composites prepared according to this set of process parameters (no. 11 in Table I) are shown in Fig. 7. The yield strength of the composites obtained using these

process parameters was 417 MPa, the tensile strength was 733 MPa, and the elongation was 35.3%. As predicted, the composite corresponding to this set of parameters showed the best overall mechanical properties of all the samples.

The tensile strength demonstrated in sample 11 was the result of a combination of the concentration and distribution of reinforcement particles, the degree of densification, and fine grain strengthening. The work of Guan et al.¹⁴ brought about a 49.4% and 38.6% increase in the yield and tensile strength of the raw material, respectively, and Jain et al.¹² increased the tensile strength by almost 10%. However, with the optimum process parameters for this work, the yield and tensile strengths of the composites were 69.5% and 36.5% higher, respectively, than without the addition of reinforcing particles. More importantly, for most earlier work, the steel matrix composites prepared were high in strength but low in elongation,^{11,12,14,39} whereas the present process retains the plasticity of the matrix material very well.

Fracture Analysis

Figure 8 shows the tensile fracture morphologies of two composites with 10 wt.% and 25 wt.% cast WC in the powder (S2 and S5). It is clear that when

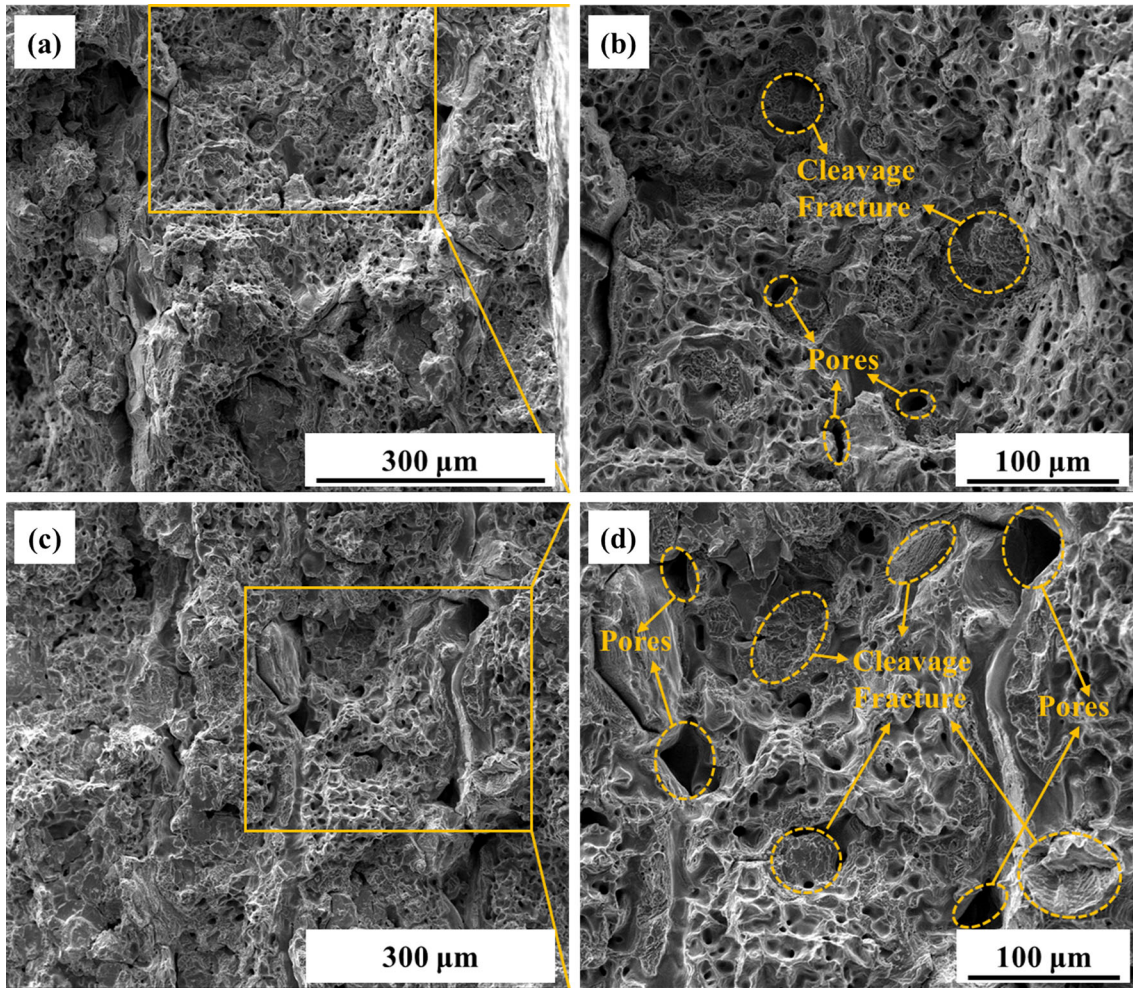


Fig. 9. Fracture profile of the material at different sintering temperatures: (a), (b) 1240 °C and (c), (d) 1280 °C.

the cast WC mass fraction was 10%, there were many dimples in the tensile fracture of the material, and the fracture mode of the material was dominated by ductile fracture. When the mass fraction of WC increased to 25%, the number of dimples in the tensile fracture decreased significantly. There were many cleavage fractures in the fracture, and the material mainly exhibited brittle fracture; this result was consistent with the elongation results of the material. Figure 8c shows the results of the EDS in the matrix region, where, not surprisingly, the element Fe was the most abundant, followed by the element Cr. This was consistent with the composition of 304, indicating that the addition of WC did not cause a vicious depletion of Cr elements in the matrix. The analysis region corresponding to Fig. 8-d was mainly at the brittle fracture feature, and the EDS results showed that the elements in this region were dominated by W, indicating that the brittle fracture in the material was mainly caused by the reinforcement particles, which further confirmed the weakening effect of the aggregation of WC particles on the plasticity of the composite.

Figure 9 shows the tensile fractures of composites sintered at 1240 °C and 1280 °C (S2 and S7). The fracture characteristics of both materials were characterized by dimples and cleavage fractures. The difference was that the fractures of materials sintered at 1240 °C were dominated by dimples, which were more numerous than those of materials sintered at 1280 °C. Therefore, the material sintered at 1240 °C exhibited mainly plastic fracture, and better plasticity than the material sintered at 1280 °C, which aligned with the tensile test results.

Figure 10 shows the fractures of two materials with different thickness reductions (S9 and S10). It can be seen from the micrographs that there were many cleavage patterns in Fig. 10a and b. The fracture also shows that the material contained many holes of varying sizes, which means that the material was not very tough. Looking at the fracture of the material with a 35% rolling reduction, Fig. 10c and d show that the holes in the material were not only reduced in number but also in size, which favored the increase in the material's tensile strength. In addition, many dimples appeared in the fracture, which also implied an increase in the

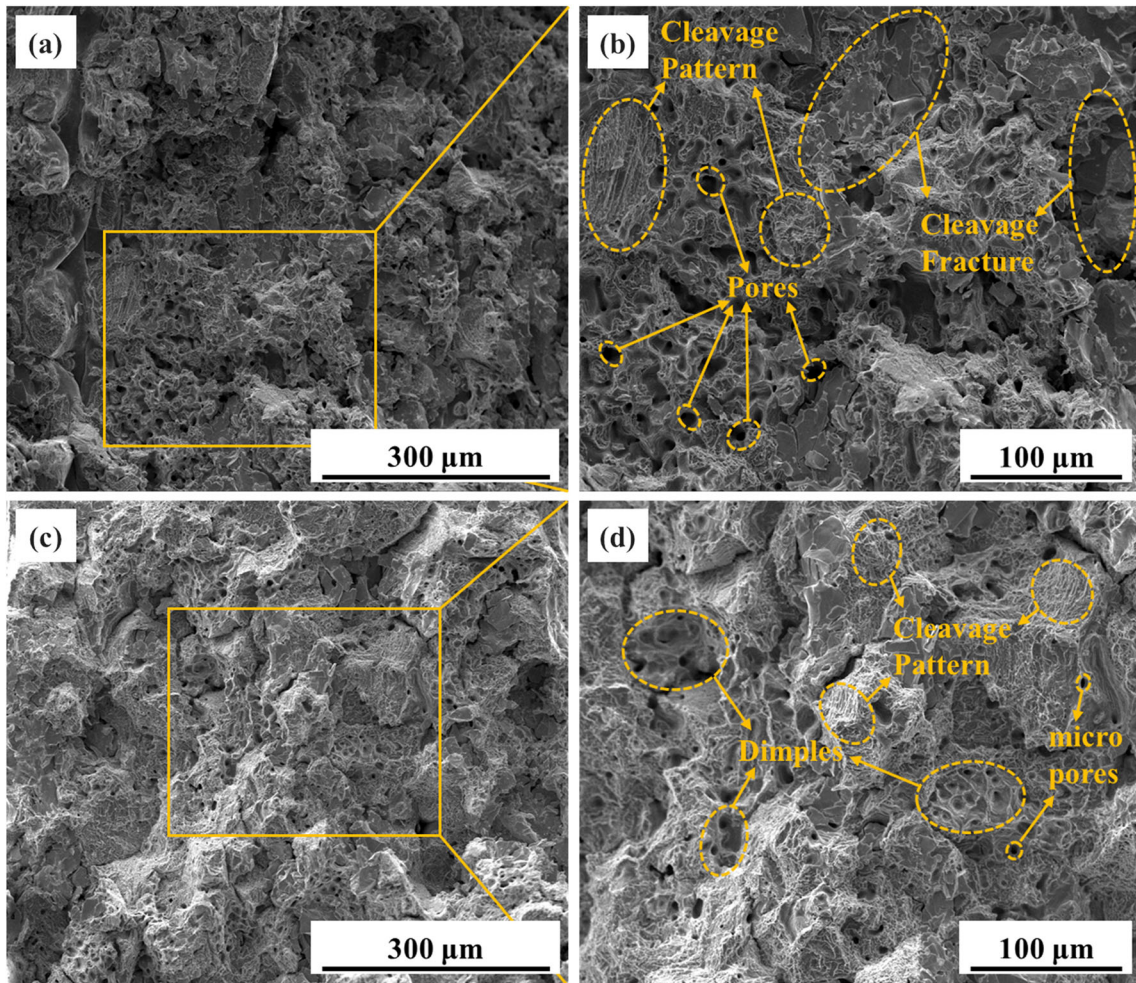


Fig. 10. Fracture profile of the material at different rolling deformations: (a), (b) 25% and (c), (d) 35%.

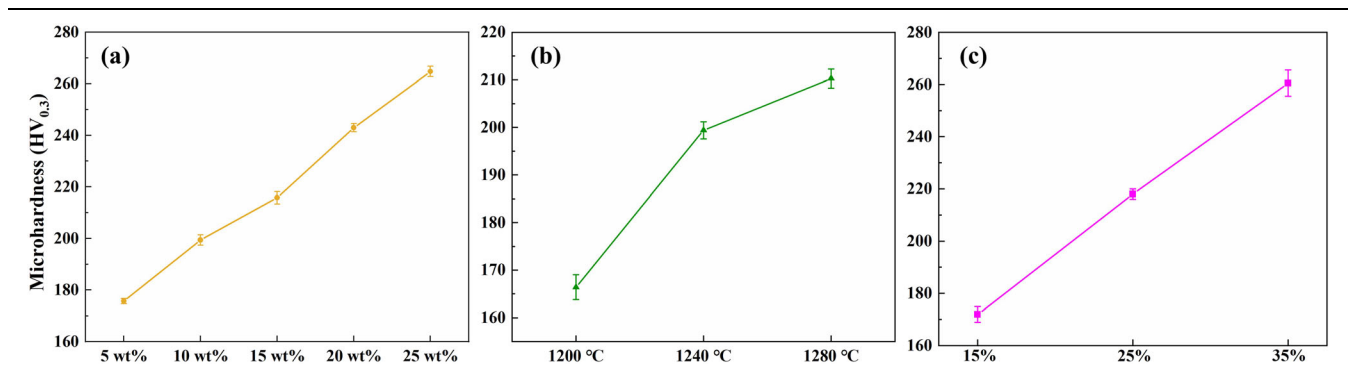


Fig. 11. Effect of process parameters on the material hardness: (a) reinforcement particle content, (b) sintering temperature, (c) rolling deformation.

toughness of the material, so the situation shown in Fig. 7 emerged: as the amount of rolling down increased, the strength and toughness of the material both appeared to increase.

Microhardness

A square specimen with a side length of 10 mm was cut from each sample to measure its microhardness. Nine evenly spaced points were selected on each example for measurement, and the average hardness of these nine points was calculated as the final hardness.

Figure 11 shows the micro-Vickers hardness of the composites, and Fig. 11a shows the hardness of the material corresponding to different cast WC contents; it can be seen that as the WC content increased, the hardness of the material also increased. The microhardness of the material was 175.68 HV when the mass fraction of cast WC in the powder was 5%, and when the content increased to 25%, the microhardness was 264.73 HV, an increase of 50.69%. This indicates that the ability of the composite material to resist deformation caused by external forces was improved. This improvement is mainly because the matrix material and the reinforcement particles jointly participate in resisting deformation when the composite material is subjected to external forces. The reinforcement particles had a greater ability to resist deformation than the matrix material, so the higher the content of reinforcement particles, the higher the overall capacity of the composite material to resist deformation. In addition, the presence of $\text{Fe}_3\text{W}_3\text{C}$ in the composite also contributed to the hardness of the material.¹⁶ Figure 11b shows the effect of sintering temperature on the hardness of the composite. It is evident that as the sintering temperature increased, the hardness of the composite increased from 166.41 HV to 210.25 HV. There were two main reasons for this phenomenon: on the one hand, as the sintering temperature increased, the quality of the metallurgical bonding within the composite increased, which made the material more resistant to external intrusion; on the other hand, the increase in sintering temperature made the material denser^{40,41} and increased the hardness of the material.⁴²

Figure 11c shows the effect of the thickness reduction on the hardness. As the rolling reduction increased from 15 to 25% to 35%, the hardness of the composite increased from 171.9 HV to 218.01 HV to 260.52 HV. The main reason for this significant improvement is that, on the one hand, the higher the rolling deformation, the higher the density of the composite material. On the other hand, cold rolling can refine the grain size and increase the strength and hardness of the material.³⁷

CONCLUSION

This paper proposes a new process for preparing cast WC particle-reinforced 304 stainless steel composites. The impacts of the process parameters on the hardness and tensile properties of the composites were investigated, and the fracture characteristics of the composites were analyzed through fracture morphology.

(1) By rolling, sintering, and then re-rolling and re-sintering, a mixed powder of cast WC and 304 stainless steel together with 304 stainless steel wire mesh, cast WC particle-reinforced 304 stainless steel composites with excellent mechanical properties could be prepared. The

reinforcement particles were uniformly distributed in the composites prepared by this technology.

- (2) The composite microhardness positively correlated with all three process parameters. The larger the reinforcement content was, the greater the hard phase content in the composite, and the greater the hardness of the material. The higher the sintering temperature was, the better the densification and bonding quality of the composite, and the greater the hardness. The impact on hardness was best for rolling deformation; when it was increased from 15% to 35%, the hardness increased from 171.9 HV to 260.52 HV, an increase of 51.56%.
- (3) The homogeneity of the reinforcing particles had a crucial influence on the tensile properties of the composite. Above a specific range, high levels of enhancer particles led to clustering. In addition, higher sintering temperatures also led to the clustering of reinforcement particles. Therefore, the tensile properties of the composite exhibit an increase followed by a decrease with increasing reinforcement particle content, and a continuous decline with increasing sintering temperature.
- (4) When the accumulation of enhancer particles was not apparent, the composite material mainly showed ductile fracture. In contrast, when the reinforcement particles gathered in large quantities, the plasticity of the material was reduced significantly due to the brittleness of the reinforcement.

ACKNOWLEDGEMENTS

This work was supported by the Guangdong Provincial Key Areas R&D Program (No. 2019B090918003).

CONFLICT OF INTEREST

The authors declare that they have no conflicts of interest.

REFERENCES

1. I.A. Ibrahim, F.A. Mohamed, and E.J. Lavernia, *J. Mater. Sci.* 26, 1137 (1991).
2. D.J. Lloyd, *Int. Mater. Rev.* 39, 1 (1994).
3. S.C. Tjong, *Mater. Sci. Eng. R Rep.* 74, 281 (2013).
4. M.D. Hayat, H. Singh, Z. He, and P. Cao, *Compos. A* 121, 418 (2019).
5. H.I. Bakan and K. Korkmaz, *Mater. Des.* 83, 154 (2015).
6. Z.F. Zhang, L.C. Zhang and Y.W. Mai, *J. Mater. Sci.* 30, 1961 (1995).
7. K.H. Lo, C.H. Shek and J.K.L. Lai, *Mater. Sci. Eng. R Rep.* 65, 39 (2009).
8. E. Pagounis and V.K. Lindroos, *Mater. Sci. Eng. A Struct. Mater: Prop. Microstruct. Process.* 246, 221 (1998).
9. N. Kang, W.Y. Ma, F.H. Li, H.L. Liao, M. Liu, and C. Coddet, *Vacuum* 154, 69 (2018).
10. R. Jamaati, M.R. Toroghinejad, H. Edris, and M.R. Salmani, *Mater. Sci. Technol.* 30, 1973 (2014).

11. R. Jamaati, M.R. Toroghinejad, and H. Edris, *Mater. Des.* 54, 168 (2014).
12. J. Jain, A.M. Kar, and A. Upadhyaya, *Mater. Lett.* 58, 2037 (2004).
13. J. Abenojar, F. Velasco, A. Bautista, M. Campos, J.A. Bas, and J.M. Torralba, *Compos. Sci. Technol.* 63, 69 (2003).
14. D.D. Guan, X.B. He, R. Zhang, and X.H. Qu, *Mater. Sci. Eng. A Struct. Mater. Prop. Microstruct. Process.* 705, 231 (2017).
15. D.D. Guan, X.B. He, R. Zhang, R. Li, and X.H. Qu, *Vacuum* 148, 319 (2018).
16. C.M. Lin, *Vacuum* 121, 96 (2015).
17. S. Dadbakhsh, R. Mertens, L. Hao, J. Van Humbeeck, and J.P. Kruth, *Adv. Eng. Mater.* 21, 18 (2019).
18. K. Das, T. Bandyopadhyay, and S. Chatterjee, *J. Mater. Sci.* 40, 5007 (2005).
19. C.L. Wu, S. Zhang, C.H. Zhang, J.B. Zhang, and Y. Liu, *Mater. Lett.* 217, 304 (2018).
20. S.W. Hu, Y.G. Zhao, Z. Wang, and Y.G.Q.C. LiJiang, *Mater. Des.* 44, 340 (2013).
21. Z.Z. Zhang, Y.B. Chen, L.L. Zuo, Y. Zhang, Y.S. Qi, K.W. Gao, H.S. Liu, and X. Wang, *Mater. Lett.* 210, 227 (2018).
22. J.M. Torralba, C.E. da Costa, and F. Velasco, *J. Mater. Process. Technol.* 133, 203 (2003).
23. K. Das, T.K. Bandyopadhyay, and S. Das, *J. Mater. Sci.* 37, 3881 (2002).
24. M.Y. Zhou, L.B. Ren, L.L. Fan, Y.W.X. Zhang, T.H. Lu, G.F. Quan, and M. Gupta, *J. Alloys Compd.* 838, 40 (2020).
25. M.J. Sohrabi, M. Naghizadeh, and H. Mirzadeh, *Arch. Civ. Mech. Eng.* 20, 124 (2020).
26. C.Z. Li and Z.Y. Zhou, *Adv. Eng. Mater.* 23, 2100585 (2021).
27. H.Y. Chen, D.D. Gu, H.M. Zhang, L.X. Xi, T.W. Lu, L. Deng, U. Kuhn, and K. Kosiba, *J. Mater. Process. Technol.* 289, 116959 (2021).
28. A. Fernandez-Guillermat, *Z. Metallk.* 78, 165 (1987).
29. S.C. Lin and Z.Y. Zhou, *Materials* 14, 15 (2021).
30. N. Chawla and Y.L. Shen, *Adv. Eng. Mater.* 3, 357 (2001).
31. C.S. Kim, K. Cho, M.H. Manjili, and M. Nezafati, *J. Mater. Sci.* 52, 13319 (2017).
32. A. Slipenyuk, V. Kuprin, Y. Milman, V. Goncharuk, and J. Eckert, *Acta Mater.* 54, 157 (2006).
33. J.Z. Wang, H.P. Tang, M. Qian, A.J. Li, J. Ma, Z.G. Xu, C.L. Li, Y. Liu, and Y. Wang, *JOM* 68, 890 (2016).
34. K. Zhao, Y. Liu, L. Huang, B. Liu, and Y.H. He, *J. Mater. Process. Technol.* 230, 272 (2016).
35. S.C. Lin, and Z.Y. Zhou, *JOM* 74, 2357 (2022).
36. M. Rahimian, N. Parvin, and N. Ehsani, *Mater. Sci. Eng. A Struct. Mater. Prop. Microstruct. Process.* 527, 1031 (2010).
37. J.L. Lv, T.X. Liang, C. Wang, and L.M. Dong, *Mater. Sci. Eng. C-Mater. Biol. Appl.* 62, 558 (2016).
38. D.G. Rodrigues, G.G.B. Maria, N.A.L. Viana, and D.B. Santos, *Mater. Charact.* 150, 138 (2019).
39. F. Velasco, N. Anton, J.M. Torralba, and J.M. RuizPrieto, *Mater. Sci. Technol.* 13, 847 (1997).
40. S. Pandya, K.S. Ramakrishna, A.R. Annamalai, and A. Upadhyaya, *Mater. Sci. Eng. A Struct. Mater. Prop. Microstruct. Process.* 556, 271 (2012).
41. S. Balaji, G. Joshi, and A. Upadhyaya, *Scr. Mater.* 56, 149 (2007).
42. H.W. Ni, H. He, G.Q. Li, and J. Liu, *J. Iron Steel Res. Int.* 15, 73 (2008).

Publisher's Note Springer Nature remains neutral with regard to jurisdictional claims in published maps and institutional affiliations.

Springer Nature or its licensor (e.g. a society or other partner) holds exclusive rights to this article under a publishing agreement with the author(s) or other rightsholder(s); author self-archiving of the accepted manuscript version of this article is solely governed by the terms of such publishing agreement and applicable law.